AJNR

Temporal Changes on Postgadolinium MR Vessel Wall Imaging Captures Enhancement Kinetics of Intracranial Atherosclerotic Plaques and Aneurysms

Abhinav Patel, Ramez N. Abdalla, Sammy Allaw, Donald R. Cantrell, Ali Shaibani, Frances Caprio, David M. Hasan, Ali Alaraj, Sean P. Polster, Timothy J. Carroll and Sameer A. Ansari

AJNR Am J Neuroradiol published online 25 July 2024
http://www.ajnr.org/content/early/2024/07/25/ajnr.A8370

Published July 25, 2024 as 10.3174/ajnr.A8370

ORIGINAL RESEARCH
NEUROVASCULAR/STROKE IMAGING

Temporal Changes on Postgadolinium MR Vessel Wall Imaging Captures Enhancement Kinetics of Intracranial Atherosclerotic Plaques and Aneurysms

Abhinav Patel, Ramez N. Abdalla, Sammy Allaw, Donald R. Cantrell, Ali Shaibani, Frances Caprio, David M. Hasan, Ali Alaraj, Sean P. Polster, Timothy J. Carroll, and Sameer A. Ansari

ABSTRACT

BACKGROUND AND PURPOSE: Analysis of vessel wall contrast kinetics (ie, wash-in/washout) is a promising method for the diagnosis and risk-stratification of intracranial atherosclerotic disease plaque (ICAD-P) and the intracranial aneurysm walls (IA-W). We used black-blood MR imaging or MR vessel wall imaging to evaluate the temporal relationship of gadolinium contrast uptake kinetics in ICAD-Ps and IA-Ws compared with normal anatomic reference structures.

MATERIALS AND METHODS: Patients with ICAD-Ps or IAs who underwent MR vessel wall imaging with precontrast, early postcontrast (5–15 minutes), and delayed postcontrast (20–30 minutes) 3D T1-weighted TSE sequences were retrospectively studied. ROIs of a standardized diameter (2 mm) were used to measure the signal intensities of the cavernous sinus, pituitary infundibulum, temporalis muscle, and choroid plexus. Point ROIs were used for ICAD-Ps and IA-Ws. All ROI signal intensities were normalized to white matter signal intensity obtained using ROIs of 10-mm diameter. Measurements were acquired on precontrast, early postcontrast, and delayed postcontrast 3D T1 TSE sequences for each patient.

RESULTS: Ten patients with 17 symptomatic ICAD-Ps and 30 patients with 34 IA-Ws were included and demonstrated persisting contrast uptake ($P < .001$) of 7.21% and 10.54% beyond the early phase (5–15 minutes postcontrast) and in the delayed phase (20–30 minutes postcontrast) on postcontrast MR vessel wall imaging. However, normal anatomic reference structures including the pituitary infundibulum and cavernous sinus demonstrated a paradoxical contrast washout in the delayed phase. In both ICAD-Ps and IA-Ws, the greatest percentage of quantitative enhancement (>70%–90%) occurred in the early phase of postcontrast imaging, consistent with the rapid contrast uptake kinetics of neurovascular pathology.

CONCLUSIONS: Using standard MR vessel wall imaging techniques, our results demonstrate the effects of gadolinium contrast uptake kinetics in ICAD-Ps and IA-Ws with extended accumulating enhancement into the delayed phase (> 15 minutes) as opposed to normal anatomic reference structures that conversely exhibit decreasing enhancement. Because these relative differences are used to assess qualitative patterns of ICAD-P and IA-W enhancement, our findings highlight the importance of standardizing acquisition time points and MR vessel wall imaging protocols to interpret pathologic enhancement for the risk stratification of cerebrovascular pathologies.

ABBREVIATIONS: AWE = aneurysm wall enhancement; IA = intracranial aneurysm; IA-W = intracranial aneurysm wall; ICAD = intracranial atherosclerotic disease; ICAD-P = intracranial atherosclerotic disease plaque; K^{trans} = volume transfer constant; SI = signal intensity; VWI = vessel wall imaging

Novel MRI techniques have been utilized to study the risk of cerebrovascular pathologies, including high resolution MR-VWI for lesion enhancement, functional MRI for contrast permeability/kinetics, and even molecular MRI for ferumoxytol uptake.[1,2] Intracranial atherosclerotic disease (ICAD) is a leading cause of acute ischemic stroke globally, with an incidence of 15%–30% in African Americans and 30%–50% in Asians.

Received December 5, 2023; accepted after revision March 5, 2024.

From the Departments of Radiology, (A.P., R.N.A., D.R.C., A.S., S.A.A.), Neurology (D.R.C., A.S., F.C., S.A.A.), and Neurological Surgery (A.S., S.A.A.), Northwestern University Feinberg School of Medicine, Chicago, Illinois; Department of Radiology (R.N.A.), Ain Shams University, Cairo, Egypt; Department of Radiology (S.A., T.J.C.), University of Chicago, Chicago, Illinois; Department of Neurological Surgery (D.M.H.), Duke University School of Medicine, Durham, North Carolina; Department of Neurological Surgery (S.P.P.), University of Chicago Pritzker School of Medicine, Chicago, Illinois; and Department of Neurosurgery, College of Medicine (A.A.), University of Illinois at Chicago, Chicago, Illinois.

Abhinav Patel and Ramez N. Abdalla had equal contribution as co-first authors.

This study was funded by National Institutes of Health grants 1R21HL130969 (S.A.A.) and 1R01NS114632 (S.A.A., T.J.C.) of the National Heart, Lung, and Blood Institute and National Institute of Neurological Disorders and Stroke.

Please address correspondence to Sameer A. Ansari, MD, PhD, Departments of Radiology, Neurology, and Neurological Surgery, Northwestern University, Feinberg School of Medicine, 676 N. St. Clair St, Suite 800, Chicago, IL 60611-2927; e-mail: s-ansari@northwestern.edu; @NURadiology

Indicates article with online supplemental data.

http://dx.doi.org/10.3174/ajnr.A8370

Intracranial aneurysms (IAs) have an incidence of approximately 2%–3%, with SAH secondary to aneurysm rupture, with a 35%–50% mortality rate.[3-5] There is evidence to suggest both ICAD[6-8] and IA[9-14] development and symptomatology may be related to focal inflammatory pathways leading to vessel wall pathology and instability. Consequently, stratifying the risk of ischemic or hemorrhagic stroke is imperative to reduce the morbidity and mortality associated with each pathology and improve patient outcomes.

Conventional luminal imaging modalities such as CTA, MRA, and DSA have been used to evaluate neurovascular pathologies such as IAs, ICAD, and intracranial dissections. While these traditional imaging techniques resolve the size, shape, and changes in lumen diameter, these are nonspecific morphologic changes characteristic of many intracranial vasculopathies that cannot differentiate imaging features of ICAD plaque or aneurysm wall stability versus instability. Multiple studies have demonstrated the potential of high-resolution MR vessel wall imaging (VWI) modalities to provide additional physiologic information of vessel wall pathology.[6] The use of MR VWI, in conjunction with luminal imaging techniques, has led to earlier detection and characterization of cerebrovascular pathologies and has aided in risk stratification.[7,8]

MR VWI with gadolinium contrast enhancement has been used as a biomarker of local ICAD plaques (ICAD-Ps) and intracranial aneurysm wall (IA-W) inflammation and permeability, associated with an increased likelihood of ischemic stroke and aneurysm rupture, respectively. Due to the interplay between inflammation and aneurysm remodeling,[9] contrast enhancement of the IA-W has been identified as a surrogate for inflammation and subsequent aneurysm growth and rupture. Marchese et al,[10] Pera et al,[11] and Kurki et al[12] have added to the growing body of evidence[1,9] suggesting that the vascular biology of ruptured IAs is distinct from unruptured IAs—in all of these studies, inflammation has been identified as a key factor in the pathway to IA rupture. Gadolinium uptake into the wall and subsequent extravasation into the extraluminal space are associated with focal instability.[2,13-15] Moreover, a similar pattern of inflammation-linked instability has been observed in ICAD-Ps.[16] Hence, MR VWI with gadolinium contrast has become an excellent tool for the quantitative evaluation of ICAD-Ps and IAs using enhancement as a biomarker of inflammation and/or increased permeability in high-risk lesions.

Traditionally, early contrast agent kinetics are evaluated with fast T1-weighted gradient-echo acquisitions. The rapid frame rates enable accurate quantification of arterial input functions and tissue curves, albeit at the expense of spatial resolution and bright blood signal. These evaluations typically require specialized acquisitions and post-processing software.[2,16,18] With the wide availability of high-resolution 3D T1-weighted TSE, VWI protocols can be used to identify contrast uptake and even delayed kinetics in the arterial wall of normal and diseased vessels for risk stratification.

Despite the wide availability of high-quality 3D T1-weighted TSE scans and the prevalence of ICAD and IAs, no standardized protocol for VWI has been established, with imaging centers using different MR scanner settings, pulse sequence techniques, and timing of image acquisitions after contrast injection.[6]

Table 1: MR-VWI parameters for ICAD-Ps and IAs

Parameter	Value
Sequence	3D TSE
Scan plane	Axial
FOV (mm)	160
TR/TE (ms)	800/28–32
BW (Hx/pixel)	370
θ	120
Acceleration	2
ETL	42
Matrix acquisition	0.5 mm × 0.5 mm
Matrix recon	0.5 mm × 0.5 mm
No. of slices/thick	120/0.5

Note:—FOV indicates field of view; TR, the repetition time; TE, the echo time; BW, bandwidth; ETL, echo train length; Matrix recon, matrix reconstruction.

Contrast timing is of particular importance because the utility of VWI is predicated on both precontrast and, more importantly, postcontrast T1-weighted sequences to characterize enhancement features associated with vessel wall inflammation.[8,17] In this article, we aimed to qualitatively and quantitatively study the temporal changes of post-contrast enhancement intensity to better understand delayed contrast kinetics of pathologic-versus-physiologic enhancement in ICAD-Ps, IAs, and normal brain structures. We aimed to use these prospective kinetic studies to assess the optimal postcontrast image-acquisition timing and improve the diagnostic and prognostic capabilities of black-blood 3D T1-weighted TSE imaging sequences.

MATERIALS AND METHODS

We performed a single-center, institutional review board–approved, retrospective chart review of patients obtained from the PACS at Northwestern Memorial Hospital, a tertiary academic medical center. We included patients presenting with ischemic symptoms (acute or subacute ischemic stroke and/or TIA) with an attributable underlying intracranial stenosis (>50%) secondary to ICAD (patients, $n = 16$; plaques, $n = 23$) or patients with IAs (patients, $n = 46$; IAs, $n = 67$) who underwent MR VWI within 2 weeks of symptoms or presentation. Both patient populations were subjected to an interim MR VWI protocol used between August 2019 and September 2020, which included both early and delayed post-contrast enhancement scans. IAs adjacent to the cavernous sinus were excluded due to the limited ability to evaluate enhancement characteristics in proximity to intense enhancement (IAs, $n = 4$). Ruptured IAs or treated IAs (IAs, $n = 7$), IAs < 2mm (IAs, $n = 17$), and fusiform aneurysms were excluded (IAs, $n = 2$). Additionally, incomplete studies and studies with poor diagnostic value due to marked motion degradation were omitted (IAs, $n = 3$; plaques, $n = 6$).

MR VWI was performed using T1-weighted 3D black-blood TSE (sampling perfection with application-optimized contrasts using variable flip angle evolutions [SPACE; Siemens]) sequences and included a precontrast and 2 postcontrast acquisitions at different time points. These time points were defined as "early" (5–15 minutes) and "delayed" (20–30 minutes) after contrast administration (0.1 mmol/kg of Gadavist; Bayer Schering Pharma). All studies were performed on a 3T MR imaging scanner (Magnetom Skyra; Siemens). Additional MR VWI protocol parameters are summarized in Table 1.

Following identification of studies that met the inclusion/exclusion criteria, qualitative and quantitative assessment of the presence and degree of contrast enhancement was performed on normal anatomic reference structures with varying physiologic enhancement and vascular characteristics (pituitary infundibulum, temporalis muscle midbelly fibrous band, cavernous sinus, and choroid plexus). Neurovascular pathology of interest (ICAD-P or IA-W) was also evaluated at both early and delayed postcontrast time points. Quantitative evaluation of the signal intensity (SI) of ICAD-P and IA-W enhancement was computed using ROIs at the site of maximum SI. For normal anatomic reference structures, the SIs of the aforementioned structures were evaluated using circular ROIs of a standardized diameter (2 mm) to serve as internal control values. For each postcontrast time point, 3 measurements were obtained for reference structures and neurovascular lesions, which were then averaged to obtain a mean SI. To account for the variances in the baseline SI of each MR imaging sequence, the mean SI of precontrast, early and delayed postcontrast images were normalized using mean precontrast, early and delayed postcontrast white matter SIs, respectively. The white matter SI was obtained using ROIs of 10 mm adjacent to the vascular lesion. In rare cases in which adjacent white matter could not be evaluated, white matter in the centrum semiovale with a ROI standardized diameter of 10 mm was used.

Normalized SI was defined as enhancement of neurovascular lesions relative to enhancement of adjacent white matter:

$$\widehat{SI} = \frac{SI_{lesion}}{SI_{adj\ \ white\ \ matter}}.$$

A neuroradiologist (R.N.A.) blinded to the clinical and imaging findings evaluated neurovascular lesions on MR VWI for subjective grading. Both ICAD-Ps and IA-Ws were assessed qualitatively, graded in binary form as "enhancing" or "nonenhancing" when comparing pre- versus postcontrast TI SPACE imaging. IAs were also measured for maximum aneurysm diameter size and graded for "regular" versus "irregular" saccular aneurysm morphology using both MR VWI and TOF-MRA imaging.

Following the descriptive statistical analysis of the data, normalized and unnormalized data were tabulated under 3 time points—precontrast, early, and delayed postcontrast—and repeated measures ANOVA was used to compare the change in enhancement statistically. SPSS, Version 29 (IBM) was used to perform all statistical analysis.

RESULTS

Patient Demographics/Comorbidities

Seventeen ICAD-Ps in 10 patients and 34 IAs in 30 patients were evaluated after inclusion and exclusion criteria were fulfilled. The mean age of patients with ICAD-Ps was 71.3 (SD, 15.3) years (range, 46–90 years), and with IA, it was 63 (SD, 11.5) years (range, 32–81years). The mean size of IAs was 5 (SD, 3) mm (range, 2–18 mm). Six of 10 patients with ICAD-Ps had MR DWI findings of acute or subacute ischemic stroke, whereas the remaining 4 patients presented with TIAs with negative findings on DWI scans. Table 2 summarizes patient demographics and screened comorbidities/vascular risk factors obtained via retrospective chart review.

Figures 1–2 show representative imaging of intracranial aneurysms and ICAD-Ps using 3D TOF-MRA and precontrast and early and/or delayed postcontrast 3D TSE sequences.

Statistical Analysis

ICAD-Ps, IA-Ws, and normal anatomic reference structures showed a statistically significant ($P < .001$) increase in normalized mean signal intensity ($\widehat{SI}$) or enhancement from precontrast to early and delayed postcontrast scans on T1 SPACE sequences. There was also a statistically significant increase in $\widehat{SI}$ or further contrast enhancement in ICAD-Ps and IA-Ws ($P < .001$) between early and delayed imaging. In contrast, there was a statistically significant decrease in $\widehat{SI}$ or relative loss of contrast enhancement in the cavernous sinus ($P < .001$) and the pituitary infundibulum ($P < .001$) from early-to-delayed imaging. The temporalis muscle and choroid plexus tissue showed no significant change in enhancement between early and delayed contrast

Table 2: Baseline patient demographics and comorbidities[a]

Comorbidities, No. (%)	ICAD-P	IA
Hypertension	8 (80.0)	17 (56.67)
Diabetes	4 (40.0)	7 (23.33)
Hyperlipidemia	7 (70.0)	14 (46.67)
Alcohol	4 (40.0)	12 (40)
Smoking	5 (50.0)	11 (36.67)
Family history	–	11 (36.67)
Vasculopathy, connective tissue disease	0 (0)	1 (3.23)
Fibromuscular dysplasia	0 (0)	2 (6.45)

Note:—The en dash indicates that family history data is unavailable.
[a] Only family history of cerebral aneurysms was obtained. ICAD-P ($n = 10$), intracranial aneurysms ($n = 30$); mean age, 71.3 (SD, 15.3) years; 62.96 (SD, 11.48) years.

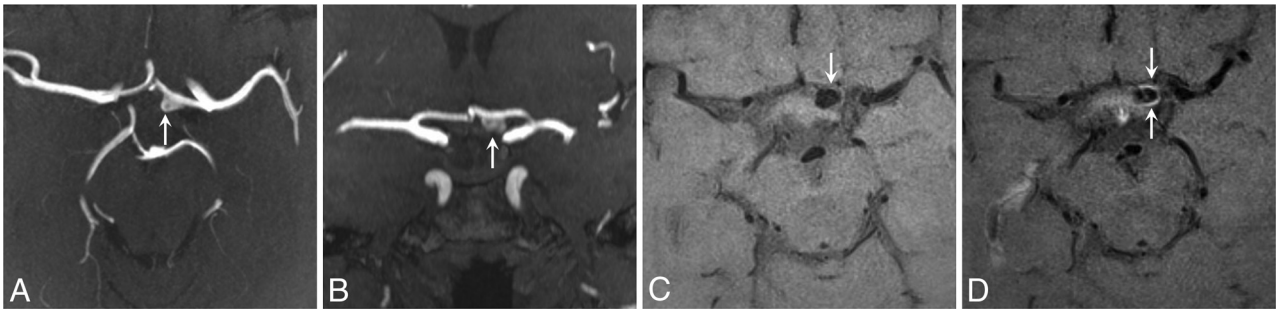

FIG 1. This series includes TOF-MRA scans (*A* and *B*) and precontrast (*C*) and postcontrast (*D*) T1-weighted 3D TSE sequences showing a 7 × 6 mm unruptured aneurysm in the left anterior cerebral artery (*arrows*). The delayed postcontrast image (*D*) reveals circumferential enhancement of the dome of the aneurysm, indicating wall instability, denoted by opposing white arrows.

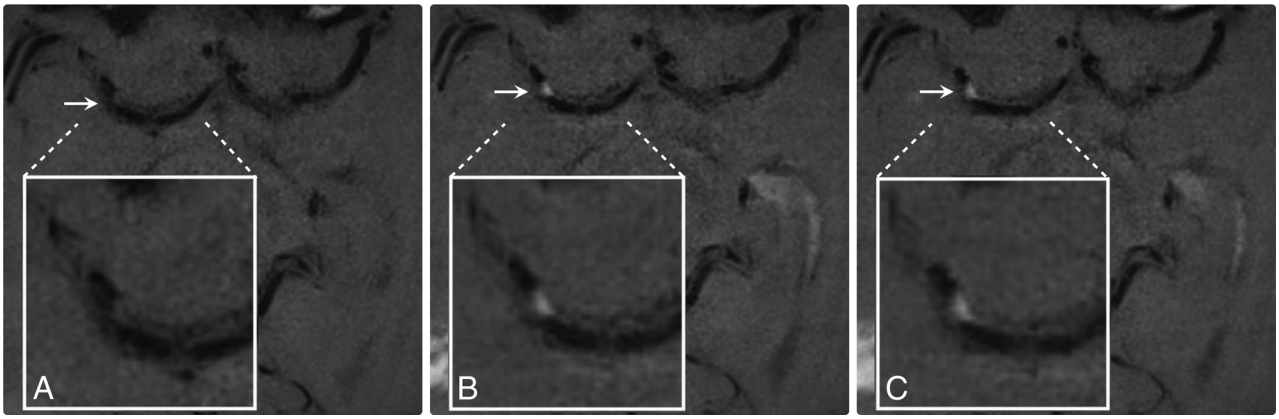

FIG 2. This series include precontrast (*A*), early postcontrast (*B*), and delayed postcontrast (*C*) T1 3D TSE sequences that demonstrates progressive enhancement of an ICAD plaque located in the right M1 segment of the right MCA in a patient presenting with an ischemic stroke in the corresponding vascular territory, suggestive of plaque instability. Note the excellent arterial blood flow (black-blood) suppression that allows focal identification of eccentric ICAD plaque enhancement (Plaques are annotated by a *white arrow* and magnified in box to demonstrate degree of enhancement in all of the above images).

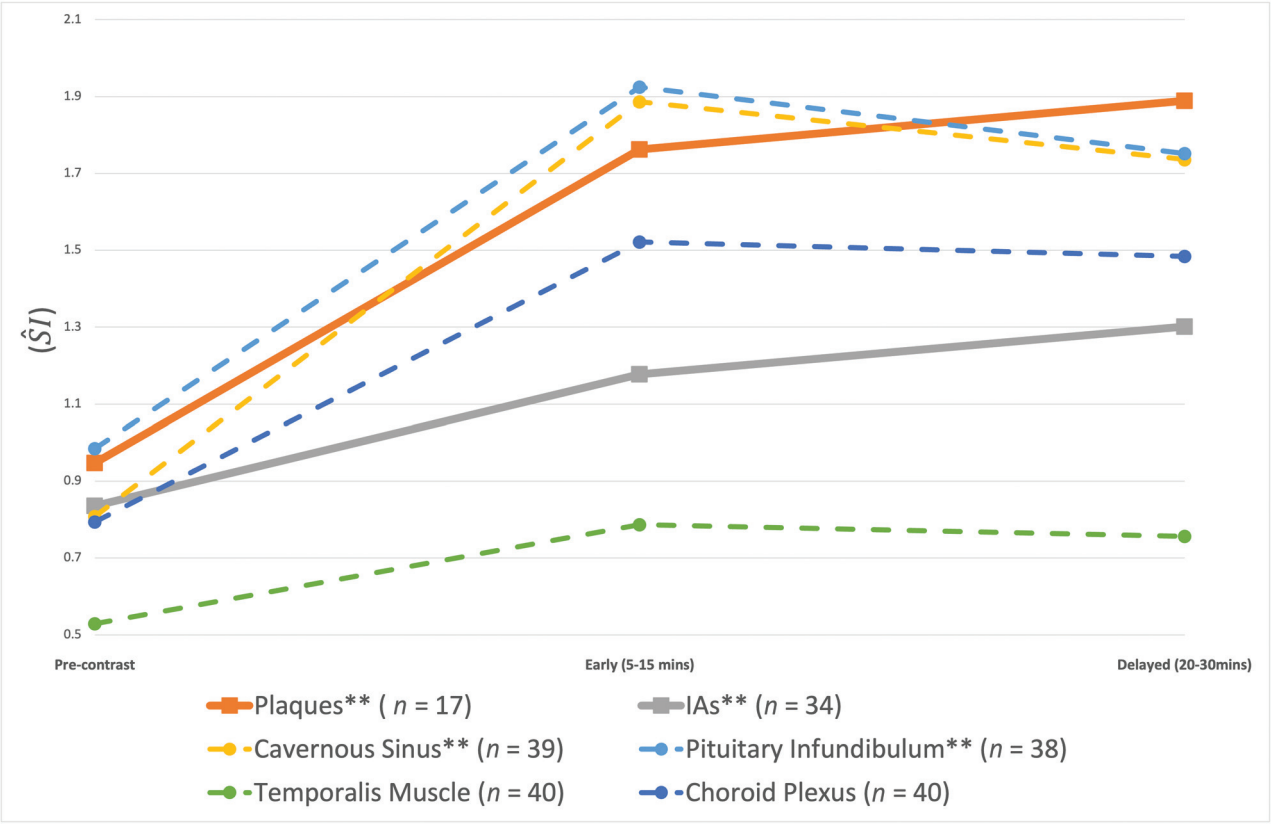

FIG 3. Temporal evolution of contrast enhancement of ICAD-Ps and IA-Ws, and normal anatomic reference structures. Double asterisks indicate $P < .05$ for early-to-delayed $\Delta(\widehat{SI})$.

phases ($P = .195$ and $P = .711$, respectively). The normalized mean $\widehat{SI}$ of both neurovascular lesions of interest (ICAD-P and IA-W) and anatomic reference structures are aggregated in Table 3. The unnormalized SI values are recorded in the Online Supplemental Data. The temporal evolution of gadolinium enhancement is plotted in Figs 3 and 4.

ICAD-Ps demonstrated a mean $\widehat{SI}$ of 0.947 before contrast administration, which increased to 1.762 on early postcontrast imaging and further increased to 1.889 on delayed imaging, a 7.21% increase in enhancement between the early and delayed phases. Following a similar trend, IAs demonstrated a mean $\widehat{SI}$ of 0.838 precontrast, increasing to 1.177 in the early phase and further increasing to 1.301 in delayed-phase imaging, indicating a 10.54% increase in $\widehat{SI}$ between the early and delayed phases.

Conversely, $\widehat{SI}$ of the pituitary infundibulum decreased from 1.925 to 1.752 (−8.99%) and that of the cavernous sinus decreased from 1.886 to 1.736 (−7.95%) between early and delayed phases, indicating contrast washout. The $\widehat{SI}$ of the temporalis muscle and

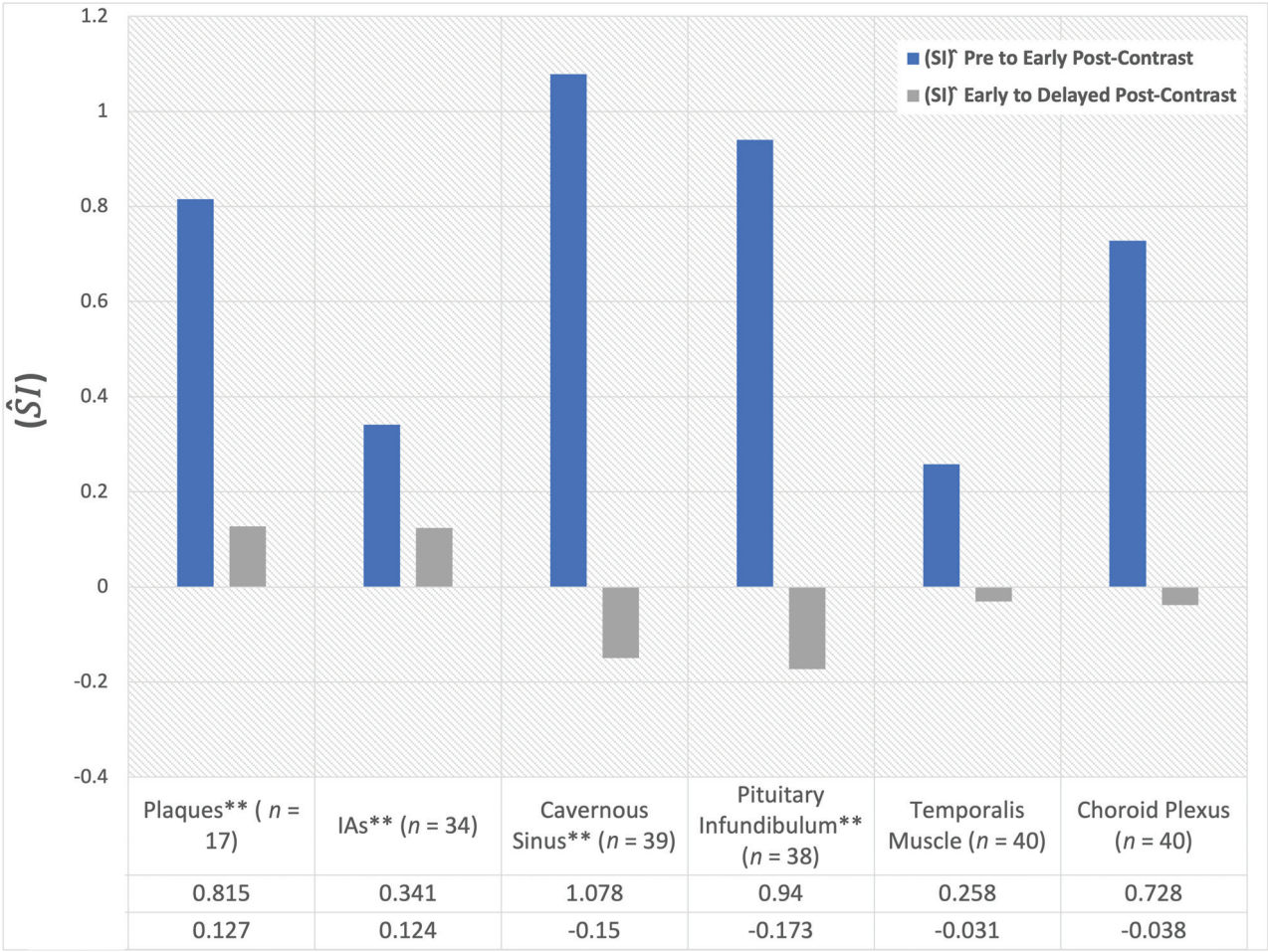

FIG 4. Temporal evolution of contrast enhancement of ICAD-Ps and IA-Ws and normal anatomic reference structures. Precontrast-to-early and early-to-delayed phase $\Delta(\widehat{SI})$, representing raw normalized changes in SI between phases. *Double asterisks* indicate $P < .05$ for early-to-delayed $\Delta(\widehat{SI})$. All precontrast-to-early changes are statistically significant and therefore not labeled.

Table 3: Normalized mean $\widehat{SI}$ and enhancement at early-versus-delayed MR VWI scanning time points

Location (No.)	Precontrast	Early (5–15 mins)	Delayed (20–30 mins)	Early to Delayed (Delayed-Early)	%Δ (% change in $\widehat{SI}$)	*P* Value
ICAD-Ps (17)	0.947	1.762	1.889	0.127	7.21%	<.001
IAs (34)	0.836	1.177	1.301	0.124	10.54%	<.001
Cavernous sinus (39)	0.808	1.886	1.736	−0.15	−7.95%	<.001
Pituitary infundibulum (38)	0.985	1.925	1.752	−0.173	−8.99%	<.001
Temporalis muscle (40)	0.529	0.787	0.756	−0.031	−3.94%	.195
Choroid plexus (40)	0.794	1.522	1.484	−0.038	−2.50%	.711
IAs <5 mm (17)	0.848	1.141	1.239	0.098	8.59%	.025
IAs >5 mm (17)	0.824	1.214	1.363	0.149	12.27%	.002
Regular (16)	0.821	1.149	1.249	0.1	8.70%	.012
Irregular (18)	0.848	1.202	1.347	0.145	10.98%	.004
No AWE (13)	0.858	0.969	1.036	0.067	0.05%	.048
AWE (21)	0.822	1.306	1.465	0.159	12.17%	.003

choroid plexus tissue minimally decreased from 0.787 to 0.756 and 1.522 to 1.484, respectively, neither of which decrease was statistically significant.

We qualitatively categorized high- versus low-risk IAs by the presence or absence of aneurysm wall enhancement (AWE), size > 5 or < 5 mm, and morphology (irregular or regular shape), respectively.[19] Irrespective of high- or low-risk IA features, a significant increase in $\widehat{SI}$ persisted from the early-to-delayed postcontrast imaging (Table 3), even in patients who qualitatively demonstrated no AWE (quantitative $\widehat{SI}$ 0.969 early versus 1.036 delayed with a 6.91% increase; $P = .048$). After we further stratified contrast enhancement by IA size (Fig 5), IA size <5 mm demonstrated a significant increase in contrast enhancement from early ($\widehat{SI}$ 1.141) to delayed ($\widehat{SI}$ 1.239) imaging with an 8.6% increase. IA size is discussed in Fig 5. Aneurysms of >5 mm exhibited a larger increase in $\widehat{SI}$ from pre- to early postcontrast

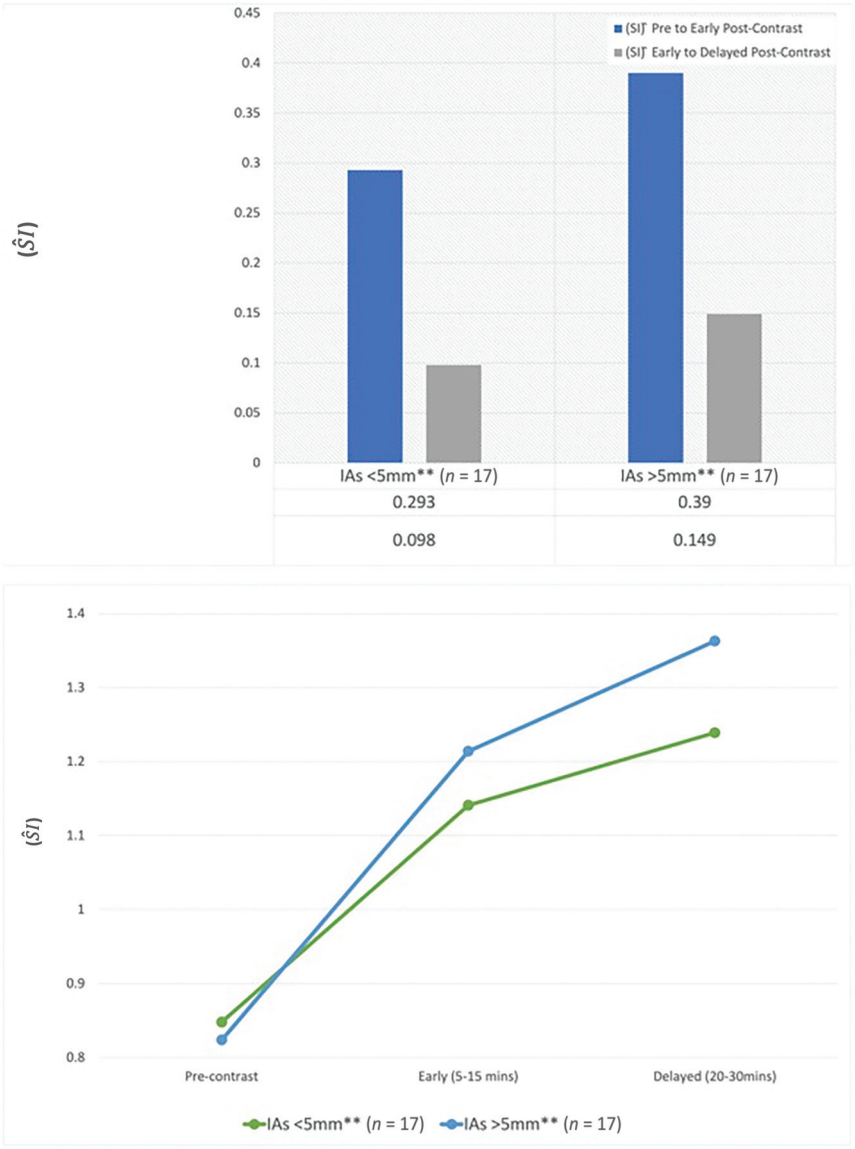

FIG 5. Kinetics of IA-Ws enhancement stratified by aneurysm size. Increase ($\widehat{SI}$) in IA wall from pre- to early postcontrast imaging correlates with aneurysm size, though a continuous increase in ($\widehat{SI}$) from early-to-delayed postcontrast imaging occurs in all aneurysms. Larger aneurysms (>5 mm) demonstrate a greater increase in ($\widehat{SI}$) on both pre- to early postcontrast imaging and early-to-delayed imaging, accounting for differential rates of contrast uptake/permeability. *Double asterisks* indicate $P < .05$ for early-to-delayed $\Delta(\widehat{SI})$.

imaging, consistent with a faster rate of contrast uptake/permeability. Although all aneurysms continue to demonstrate increasing $\widehat{SI}$ from early to delayed postcontrast imaging, this increase is more prominent in smaller aneurysms (<5 mm), reaching steady-state levels after a relatively slower rate of contrast uptake, suggesting differential contrast uptake kinetics in high- versus low-risk aneurysms by size.

DISCUSSION

Our MR VWI study indicates that symptomatic ICAD-Ps and IA-Ws accumulate gadolinium contrast beyond the early-phase (5–15 minutes) imaging with contrast uptake/permeability continuing into the delayed phase (20–30 minutes). de Havenon et al[20] reported similar findings in their study of enhancement of ICAD-Ps that demonstrated the highest degree of enhancement in the cohort correlated with the longest duration between contrast injection and image acquisition. However, this temporal enhancement pattern was not corroborated in the same patients across time and prompted us to transiently alter our MR VWI imaging protocols between August 2019 and September 2020. Because we studied this phenomenon for any clinical impact, we performed a retrospective institutional review board–approved study to quantitatively assess these temporal enhancement patterns of ICAD-Ps and IA-Ws in comparison with normal anatomic reference structures.

High-resolution black-blood MR VWI techniques are being increasingly adopted to clinically diagnose and stratify the risk of various neurovascular pathologies, notably ICAD-Ps and IA-Ws (cerebral aneurysm), without the need for functional MR imaging and specialized postprocessing software for dynamic contrast enhancement–based permeability techniques used in the research domain.[15,16,18] By means of standard black-blood T1-weighted 3D TSE sequences, imaging findings of T1-hyperintense signal abnormality and/or contrast enhancement of ICAD-Ps or IA-Ws can suggest unstable neurovascular pathology. In fact, MR VWI postcontrast enhancement may provide an imaging biomarker of focal inflammation, neoangiogenesis, and/or increased permeability found in the pathogenesis of symptomatic ruptured ICAD-Ps or thin-walled IA-Ws. Previous studies have established the histologic correlation between macrophage-mediated inflammation of atherosclerotic plaques and early-phase (5–15 minutes) contrast absorption. More advanced functional MR imaging studies have examined the correlation between macrophage infiltration of carotid atherosclerotic plaques with the volume transfer constant (K^{trans}),[2,21] a quantitative measure of the permeability across the vascular wall, with Kerwin et al[21] computing the correlation between K^{trans} and macrophage concentration at $r = 0.75$.[2] Because K^{trans} determines a transfer rate of contrast from the intravascular lumen to the extravascular extracellular space, we hypothesize that the continued absorption into the delayed phase in ICAD-Ps and IAs is related to accumulation of contrast extraluminally. Vakil et al[16,18] demonstrated that similar contrast uptake kinetic measurements of K^{trans} can also be acquired from ICAD-Ps and IA-Ws and that increased K^{trans} permeability was

associated with symptomatic ICAD-Ps and high-risk cerebral aneurysms.[16,18]

It is unclear whether contrast enhancement is limited to the inflammatory state of symptomatic unstable ICAD-Ps or IA-Ws, because confounding mechanisms may include neoangiogenesis or endothelial dysfunction/permeability. Computational fluid dynamics studies maintain that hemodynamic conditions lead to altered wall shear stress, which, in turn, leads to recruitment of invading macrophages through monocyte chemoattractant protein-1 expression.[22] However, regardless of the cause of IA inflammation, inflammation plays a central role in chronic endothelial dysfunction and intramural pathology, with both ICAD-Ps and IA-Ws demonstrating persistent leakage of gadolinium contrast into the delayed phase.

In this study, our goal was to explore the temporal enhancement of ICAD-Ps and IA-Ws in the early and delayed phases on postcontrast MR VWI sequences and derive insight into the optimal timing for image-acquisition postcontrast infusion and any diagnostic impact relative to normal anatomic reference structures. We discovered that >70%–90% of contrast enhancement of both neurovascular pathologies occurs in the early phase (5–15 minutes), but contrast uptake and accumulation indeed continue into the delayed phase (20–30 minutes). Furthermore, early contrast kinetics are integral to capturing the rate and variability of pathologic contrast enhancement as suggested even in our study when stratifying high-risk, >5 mm IAs, suggesting that optimum clinical MR VWI protocols should initiate postcontrast scanning immediately after gadolinium infusion in the early phase.

Finally, the pituitary infundibulum is the most commonly used reference structure for the qualitative grading of enhancement in ICAD-Ps and IA-Ws.[23,24] As shown in Fig 1, the $\widehat{SI}$ increase in ICAD-Ps mimics the rise of the pituitary stalk between the precontrast and early-phase postcontrast imaging. However, unlike the pituitary stalk and other normal anatomic reference structures, ICAD-Ps and IA-Ws show a unique feature of gradual contrast uptake and continuous enhancement into the delayed phase. Because these reference structures exhibit paradoxical contrast washout (renal excretion) in the delayed phase with a drop in signal intensity, this can artificially elevate the qualitative enhancement grading of ICAD-Ps and IA-Ws relative to the pituitary stalk. Furthermore, smaller <5 -mm IAs may have decreased contrast uptake compared with high-risk, larger >5-mm IAs or symptomatic ICAD-Ps in the early phase (Fig 5) but then accumulate contrast in the delayed phase, limiting the diagnostic differentiation, qualitatively and quantitatively, in the delayed phase.

Our study had several limitations, including a small sample size of patients, especially with ICAD-Ps, that could affect the generalizability of the findings. Second, this was a single-center retrospective study with inherent bias of an MR VWI protocol that was transiently evaluated for a year, and it would be difficult to augment or reproduce these data without a formal prospective study. The lack of extended follow-up data and patient outcomes in our study limits the assessment of the frequency and impact of clinically relevant changes with time. Additionally, the data for both ICAD-Ps and IAs were restricted to mostly symptomatic lesions because patients were selected for follow-up MR VWI imaging on the basis of a symptomatic clinical picture or to guide conservative-versus-therapeutic interventions. Therefore, the asymptomatic ICAD-Ps were not evaluated and attempts at stratifying IAs into high-risk and low-risk groups on the basis of morphology and other factors may not yield demonstrable differences in contrast kinetics. Finally, our study was limited to postcontrast image acquisitions at 2 time intervals, early (5–15 minutes) and delayed (20–30 minutes), restricting the evaluation of contrast dynamics across a longer duration. Overall, a prospective multicenter study with both symptomatic and asymptomatic cerebrovascular pathologies preferably with a greater number of serial postcontrast T1-weighted 3D TSE sequences should be undertaken to minimize bias and enhance generalizability to better assess the peak time of enhancement and its correlation with clinical outcomes, and it would help with the issue of standardization in MR VWI protocols.

CONCLUSIONS

Our results suggest that ICAD-Ps and IA-Ws demonstrate continuous temporal enhancement on MR VWI by accumulating gadolinium contrast from the early into the delayed phases, probably related to pathologic leakage/permeability across time. The contrast kinetics of these neurovascular pathologies suggest that delayed-phase imaging (>15 minutes) could be misleading and demonstrate nonspecific enhancement in most ICAD-Ps and IA-Ws, especially relative to normal anatomic reference structures that exhibit paradoxical contrast washout on delayed imaging. MR VWI protocols should be standardized with postcontrast imaging acquired as soon as possible after gadolinium infusion to optimize the diagnostic accuracy in risk stratification of neurovascular pathology.

Data Availability Statement

The raw data supporting the findings of this study are available from the corresponding author on reasonable request.

Disclosure forms provided by the authors are available with the full text and PDF of this article at www.ajnr.org.

REFERENCES

1. Hasan D, Chalouhi N, Jabbour P, et al. **Early change in ferumoxytol-enhanced magnetic resonance imaging signal suggests unstable human cerebral aneurysm: a pilot study.** *Stroke* 2012;43:3258–65 CrossRef Medline
2. Kerwin WS, O'Brien KD, Ferguson MS, et al. **Inflammation in carotid atherosclerotic plaque: a dynamic contrast-enhanced MR imaging study**. *Radiology* 2006;241:459–68 CrossRef Medline
3. Wang Y, Meng R, Liu G, et al. **Intracranial atherosclerotic disease.** *Neurobiol Dis* 2019;124:118–32 CrossRef Medline
4. Vlak MH, Algra A, Brandenburg R, et al. **Prevalence of unruptured intracranial aneurysms, with emphasis on sex, age, comorbidity, country, and time period: a systematic review and meta-analysis.** *Lancet Neurol* 2011;10:626–36 CrossRef Medline
5. Wiebers DO, Whisnant JP, Huston J, 3rd, et al. **Unruptured intracranial aneurysms: natural history, clinical outcome, and risks of surgical and endovascular treatment.** *Lancet* 2003;362:103–10 CrossRef
6. Song JW, Moon BF, Burke MP, et al. **MR intracranial vessel wall imaging: a systematic review.** *J Neuroimaging* 2020;30:428–42 CrossRef Medline

7. Young CC, Bonow RH, Barros G, et al. **Magnetic resonance vessel wall imaging in cerebrovascular diseases.** *Neurosurg Focus* 2019;47:E4 CrossRef Medline
8. Alexander MD, Yuan C, Rutman A, et al. **High-resolution intracranial vessel wall imaging: imaging beyond the lumen.** *J Neurol Neurosurg Psychiatry* 2016;87:589–97 CrossRef Medline
9. Frösen J, Piippo A, Paetau A, et al. **Remodeling of saccular cerebral artery aneurysm wall is associated with rupture: histological analysis of 24 unruptured and 42 ruptured cases**. *Stroke* 2004;35:2287–93 CrossRef Medline
10. Marchese E, Vignati A, Albanese A, et al. **Comparative evaluation of genome-wide gene expression profiles in ruptured and unruptured human intracranial aneurysms.** *J Biol Regul Homeost Agents* 2010;24:185–95 Medline
11. Pera J, Korostynski M, Krzyszkowski T, et al. **Gene expression profiles in human ruptured and unruptured intracranial aneurysms.** *Stroke* 2010;41:224–31 CrossRef Medline
12. Kurki MI, Häkkinen SK, Frösen J, et al. **Upregulated signaling pathways in ruptured human saccular intracranial aneurysm wall: an emerging regulative role of toll-like receptor signaling and nuclear factor-κB, hypoxia-inducible factor-1A, and ETS transcription factors**. *Neurosurgery* 2011;68:1667–76 CrossRef Medline
13. Vergouwen MD, Backes D, van der Schaaf IC, et al. **Gadolinium enhancement of the aneurysm wall in unruptured intracranial aneurysms is associated with an increased risk of aneurysm instability: a follow-up study.** *AJNR Am J Neuroradiol* 2019;40:1112–16 CrossRef Medline
14. Wang G, Xian Wen L, Lei S, et al. **Wall enhancement ratio and partial wall enhancement on MRI associated with the rupture of intracranial aneurysms.** *J Neurointerv Surg* 2017;10:566–70 CrossRef Medline
15. Gariel F, Ben Hassen W, Boulouis G, et al. **Increased wall enhancement during follow-up as a predictor of subsequent aneurysmal growth.** *Stroke* 2020;51:1868–72 CrossRef Medline
16. Vakil P, Elmokadem AH, Syed FH, et al. **Quantifying intracranial plaque permeability with dynamic contrast-enhanced MRI: a pilot study.** *AJNR Am J Neuroradiol* 2016;38:243–49 CrossRef Medline
17. Matouk CC, Mandell DM, Günel M, et al. **Vessel wall magnetic resonance imaging identifies the site of rupture in patients with multiple intracranial aneurysms**. *Neurosurgery* 2013;72:492–96; discussion 496 CrossRef Medline
18. Vakil P, Ansari SA, Cantrell CG, et al. **Quantifying intracranial aneurysm wall permeability for risk assessment using dynamic contrast-enhanced MRI: a pilot study.** *AJNR Am J Neuroradiol* 2015;36:953–59 CrossRef Medline
19. Lindgren AE, Koivisto T, Björkman J, et al. **Irregular shape of intracranial aneurysm indicates rupture risk irrespective of size in a population-based cohort**. *Stroke* 2016;47:1219–26 CrossRef Medline
20. de Havenon A, Muhina HJ, Parker DL, et al. **Effect of time elapsed since gadolinium administration on atherosclerotic plaque enhancement in clinical vessel wall MR imaging studies.** *AJNR Am J Neuroradiol* 2019;40:1709–11 CrossRef Medline
21. Kerwin WS, Oikawa M, Yuan C, et al. **MR imaging of adventitial vasa vasorum in carotid atherosclerosis.** *Magn Reson Med* 2008;59:507–14 CrossRef Medline
22. Frösen J, Cebral J, Robertson AM, et al. **Flow-induced, inflammation-mediated arterial wall remodeling in the formation and progression of intracranial aneurysms**. *Neurosurg Focus* 2019;47:E21 CrossRef Medline
23. Qiao Y, Zeiler SR, Mirbagheri S, et al. **Intracranial plaque enhancement in patients with cerebrovascular events on high-spatial-resolution MR images.** *Radiology* 2014;271:534–42 CrossRef Medline
24. Lindenholz A, van der Kolk AG, Zwanenburg JJ, et al. **The use and pitfalls of intracranial vessel wall imaging: how we do it.** *Radiology* 2018;286:12–28 CrossRef Medline